Stabilising the Boat Conformation of Piperazines Coordinated to Iron(II): i Butyl Substituents Lead to Robust Oxidation Catalysts Via Hyperconjugation

Christian Limberg, Marc Ostermeier, Christian Herwig, Burkhard Ziemer

▶ **To cite this version:**

Christian Limberg, Marc Ostermeier, Christian Herwig, Burkhard Ziemer. Stabilising the Boat Conformation of Piperazines Coordinated to Iron(II): i Butyl Substituents Lead to Robust Oxidation Catalysts Via Hyperconjugation. Journal of Inorganic and General Chemistry / Zeitschrift für anorganische und allgemeine Chemie, 2009, 635 (12), pp.1823. 10.1002/zaac.200900275 . hal-00512581

HAL Id: hal-00512581
https://hal.science/hal-00512581

Submitted on 31 Aug 2010

HAL is a multi-disciplinary open access archive for the deposit and dissemination of scientific research documents, whether they are published or not. The documents may come from teaching and research institutions in France or abroad, or from public or private research centers.

L'archive ouverte pluridisciplinaire **HAL**, est destinée au dépôt et à la diffusion de documents scientifiques de niveau recherche, publiés ou non, émanant des établissements d'enseignement et de recherche français ou étrangers, des laboratoires publics ou privés.

Zeitschrift für Anorganische und Allgemeine Chemie

Stabilising the Boat Conformation of Piperazines Coordinated to Iron(II): i Butyl Substituents Lead to Robust Oxidation Catalysts Via Hyperconjugation

Journal:	*Zeitschrift für Anorganische und Allgemeine Chemie*
Manuscript ID:	zaac.200900275.R1
Wiley - Manuscript type:	Article
Date Submitted by the Author:	08-Jul-2009
Complete List of Authors:	Limberg, Christian; Humboldt-Universität Berlin, Institut für Chemie Ostermeier, Marc; Humboldt-Universität Berlin, Institut für Chemie Herwig, Christian; Humboldt-Universität Berlin, Institut für Chemie Ziemer, Burkhard; Humboldt-Universität Berlin, Institut für Chemie
Keywords:	Conformation, Density functional calculations, Oxidation catalysis, Iron, Tetradentate ligands

scholarONE™ Manuscript Central

Stabilising the Boat Conformation of Piperazines Coordinated to Iron(II): *i*-Butyl Substituents Lead to Robust Oxidation Catalysts Via Hyperconjugation

Marc Ostermeier,[a] Christian Limberg,*[a] Christian Herwig,[a] Burkhard Ziemer[a]

* *Prof. Dr. C. Limberg*

E-mail: christian.limberg@chemie.hu-berlin.de

[a] Institut für Chemie, Humboldt-Universität zu Berlin, Brook-Taylor-Straße 2, 12489 Berlin, Germany

Dedicated to Prof. Martin Jansen on the Occasion of his 65th birthday

Keywords: Conformation; Density functional calculations; Iron; Oxidation catalysis; Tetradentate ligands

Abstract

A known route to diastereomerically pure diketopiperazines starting from natural amino acids was utilised for the preparation of a chiral, 2,5-di-*i*-butyl substituted 1,4-bis(2-pyridyl-methyl)piperazine, which can serve as a ligand in metal complexes. While it should be possible to extend the procedure described also to derivatives with other amino acid-derived substituents in the 2,5 positions, here two bulky *i*-butyl residues were chosen with the aim of stabilising a tetradentate coordination mode at Fe^{II} centres thus avoiding coordination polymers. Reaction of the corresponding ligand $^{2i\text{-Bu}}$BPMP with $FeCl_2$ and $Fe(OTf)_2$ indeed led to the desired complexes ($^{2i\text{-Bu}}$BPMP)FeX_2 (X = Cl, OTf) with the piperazine ring in a boat conformation, as confirmed by single crystal X-ray diffraction analysis. However, unexpectedly the bulky *i*-butyl residues were found in the axial positions. To explain this phenomenon DFT calculations were carried out. The results showed that the most stable conformations of the free ligand contain the piperazine ring in a boat conformation with carbon atoms at the tips of the boat since repulsive interactions between the lone-pairs at the N atoms are avoided thereby. This way the ligand is preorganised to adopt the observed conformation with the axial *i*-butyl residues after complexation with iron(II). Moreover, it turned out that the resulting complex structures are also favoured thermodynamically over the corresponding ones with the residues in equatorial positions. Having thus stabilised the tetrapodal binding of a BPMP ligand to single iron centres, the potential of the complexes as catalysts for the oxidation of hydrocarbons with H_2O_2 was tested employing cyclooctene as a representative example. It turned out that the two complexes mentioned above show similar (moderate) activities which are comparable to those displayed by corresponding complexes of other polydentate pyridylmethyl-amino ligands. Interestingly, the two complexes described here are superior to an $Fe(OTf)_2$ complex of the unsubstituted ligand.

Introduction

Among the non-heme iron enzymes one of the best-studied classes is the one that oxygenates organic substrates. Their reaction mechanisms can be very different form case to case and for some of these proteins FeOOH intermediates were postulated [1,2]. This has led to the development of biomimetic iron complexes, which have proved effective catalysts for the oxidation of hydrocarbons with H_2O_2, and it has been shown that particularly active systems are obtained when polydentate pyridylmethylamino ligands such as those displayed in Chart 1 are employed [3].

The potential of such ligands has very recently been highlighted by work of C. White and co-workers who employed the complex shown in Chart 2 as oxidation catalyst for the stereoselective hydroxylation of aliphatic substrates by H_2O_2; the ligand employed is a chiral derivative of the well-exploited BPMEN (N,N'-dimethyl-N,N'-bis(2-pyridyl-methyl)ethylenediamine) (Chart 1) [4].

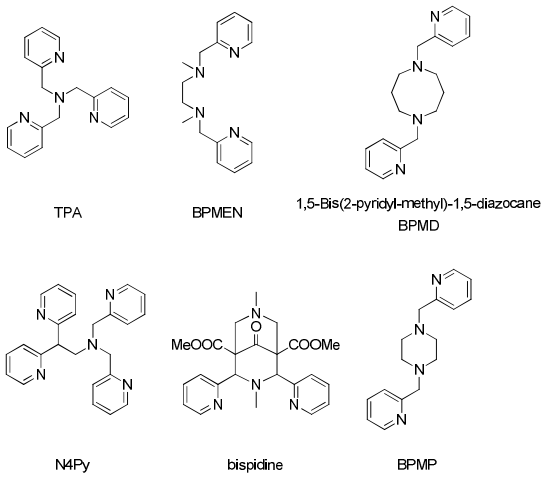

Chart 1. Ligands used in catalytic oxidation reactions.

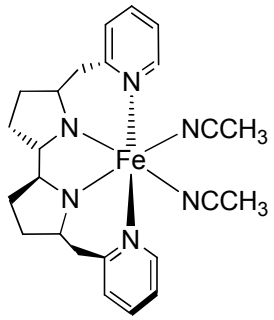

Chart 2.

Results and Discussion

We recently set out [5] investigating the iron coordination chemistry of 1,4-bis(2-pyridyl-methyl)piperazine (BPMP) [6], which is related to BPMD (see Chart 1), but the decrease of the ring-size from 8 to 6 has massive consequences for coordination chemistry: In fact, the piperazine ring of BPMP often adopts the chair conformation, not only in the free form but also in complexes [6]; it then does not act as a tetrapodal ligand but as a double bidentate ligand binding to two metal centres at the same time and this leads to polymers, which are not desirable bearing in mind catalysis. The goal of our previous studies was therefore to exploit the principal binding behaviour of BPMP to iron, hoping to reveal conditions where BPMP acts as a tetrapodal ligand for this metal. While iron(III) was found to prefer the tetradentate coordination mode due to its smaller ionic radius, the employment of iron(II)halides led to the formation of the undesired coordination polymers, which precipitate. They can only be dissolved in very polar, coordinating solvents, as these break up the polymers into dinuclear compounds containing these solvents as ligands [5,7]. However, the employment of $Fe(OTf)_2$ allowed for the isolation of a corresponding complex [(BPMP)$Fe(OTf)_2$], **I**, with BPMP binding via all of its four N donor functions according to a single crystal X-ray diffraction analysis [5]. This of course refers only to the solid state, while in solution other species can be present in addition, and the tendency of piperazine to adopt the chair conformation as found in case of the halides, exhorts to remain sceptical in this respect. We have therefore contemplated the intrinsic stabilisation of the boat conformation by the introduction of sterically demanding residues in the 2- and 5-positions: if the corresponding substituted C atoms had identical stereo configurations (*S*,*S* or *R*,*R*), the only conformation, which is free of 1,3-diaxial repulsions, would be the boat form A (Scheme 1), while a chair configuration would lead to two 1,3-diaxial interactions. Finally the boat form C was expected to be the least stable conformation.

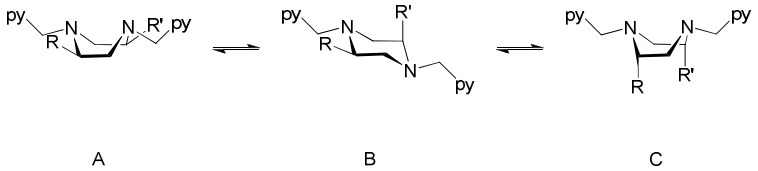

Scheme 1. Boat and chair conformations of a substituted BPMP.

Hence, such a substitution was anticipated to stabilise the boat conformation and thus the tetrapodal binding mode of the corresponding potential ligand. For its realisation an elegant synthesis for “sterically pure diketopiperazines” developed by D. E. Nitecki et al. was utilised, which sets out with natural amino acids, whose residues finally turn into residues at the piperazine unit [8]. Ideal substituents would have been *t*-butyl groups but, since there is no corresponding natural amino acid available, we employed leucine, which introduces *i*-butyl residues. A condensation reaction of the N- and O-protected leucine led to the dipeptide Boc-*S*-Leu-*S*-Leu-OMe, and after elimination of the protection groups to the cyclo-dipeptide *cyclo*-*S*-Leu-*S*-Leu was obtained [8], which was then reduced to *cis*-2,5-di-*i*-butylpiperazine [9], via treatment with $NaBH_4$/$TiCl_4$ (Scheme 2). Finally the 2-pyridyl-methyl donor functions were introduced as before in case of BPMP. After purification by means of column chromatography the diastereomerically pure potential ligand $^{2i\text{-}Bu}$BPMP was obtained, and it may be emphasized that also other chiral ligands should be accessible via this route

employing other amino acids (the meaning of this is exemplified by the above-mentioned work by White et al.).

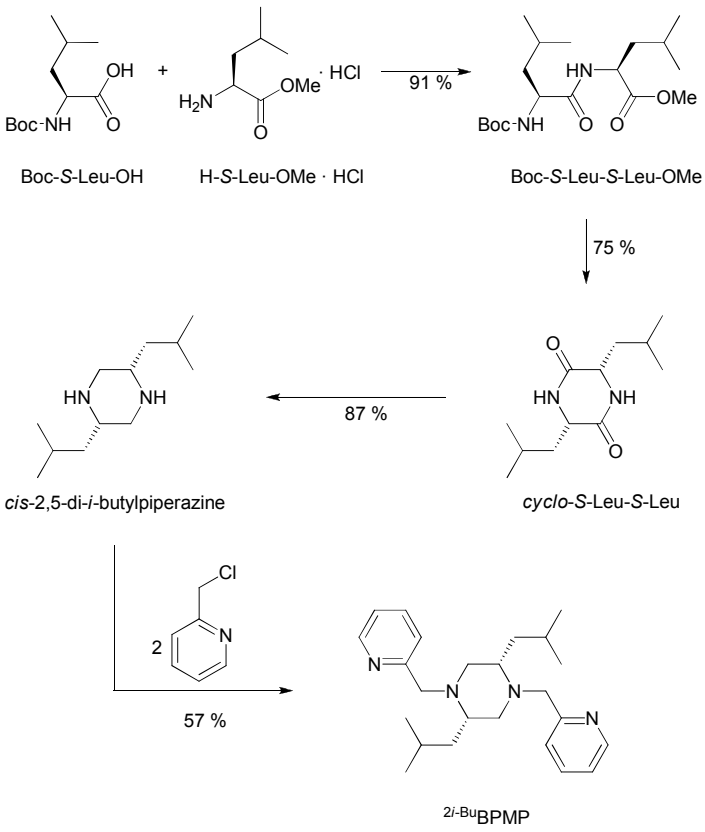

Scheme 2. Synthesis of $^{2i\text{-Bu}}$BPMP.

A convincing evidence for the success of the chosen strategy illustrated above would be the finding that on employment of $^{2i\text{-Bu}}$BPMP even with iron(II)halides mononuclear complexes are formed.

Addition of a colourless solution of $FeCl_2$ in acetonitrile to equimolar amounts of $^{2i\text{-Bu}}$BPMP dissolved in the same solvent led to an orange-coloured solution. The fact that – in contrast to the corresponding reaction with BPMP – the formation of a precipitate was not observed, already argued against a coordination polymer as the product. Slow evaporation of the solvent from a saturated acetonitrile solution led to large single crystals, and a X-ray diffraction study revealed it as [($^{2i\text{-Bu}}$BPMP)Fe(Cl)$_2$], **1** (Scheme 3). The molecular structure is depicted in Figure 1.

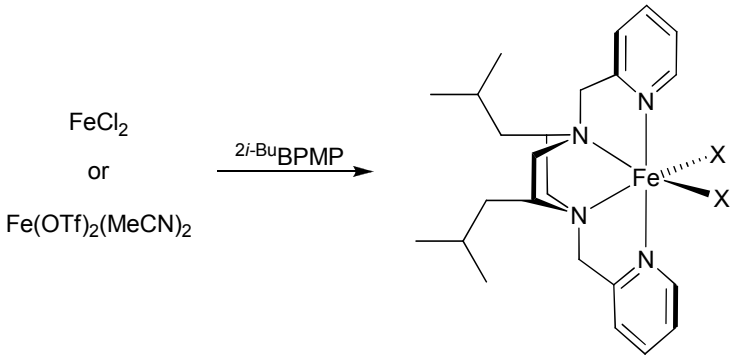

1: X = Cl
2: X = OTf

Scheme 3. Synthesis of [($^{2i\text{-Bu}}$BPMP)Fe(Cl)$_2$], **1**, and [($^{2i\text{-Bu}}$BPMP)Fe(OTf)$_2$], **2**.

As envisioned, **1** represents a mononuclear compound where the piperazine ring adopts a boat configuration, so that all four N atoms coordinate to the Fe^{II} centre together with the chloride ligands. However, in sharp contrast to the expectation the *i*-butyl residues are not found in the equatorial but in the axial positions – hence, the strategy pursued had been successful but obviously for other reasons than those envisioned. The symmetry of the coordination polyhedron is so low that it is not reasonable to assign it either a distorted octahedron or a prism. While the two triflate ligands in [(BPMP)Fe(OTf)$_2$], **I**, are positioned almost *trans* to each other (O1-Fe-O2: 169.33(4)°) [5], the corresponding Cl-Fe-Cl angle in **1** is somewhat smaller (127.37(3)°) and thus more similar to the one found in the iron(III) analogue [(BPMP)Fe(Cl)$_2$]$^+$ (134.75(4)°) [5]. Also the other structural parameters of **1** are quite similar to the ones found for this iron(III) complex, the most striking differences being found – not surprisingly – for the Fe-N bond lengths. An obvious question was now whether this result is unique, and what alterations occur, if Fe(OTf)$_2$ is employed in the complexation reaction.

Performing an analogous reaction with Fe(OTf)$_2$(CH$_3$CN)$_2$ yielded in [($^{2i\text{-Bu}}$BPMP)Fe(OTf)$_2$], **2**, as the product (Scheme 3), and its molecular structure (Figure 2) is principally very similar to the one found for **1**, the most striking difference being the widening of the X-Fe-X angle from 127.37(3)° in **1** to 155.67(7)° in **2**. Again, the *i*-butyl residues are found in the axial positions, so that this conformation generally seems to be more stable. In order to find out the origin of this surprising result DFT calculations (B3LYP/6-31G*) were carried out, which in the first step addressed the uncomplexed $^{2i\text{-Bu}}$BPMP molecule. By varying the starting geometries several local minima on the potential energy surface were determined, and indeed due to the *i*-butyl residues boat and twist conformations are preferred over the chair conformation (see Figure 3). However, in contrast to the drawings in Scheme 1 the tips within the boat structures do not correspond to the N atoms but to C atoms, so that both the *i*-butyl residues *and* the lone-pairs at the N atoms are located in equatorial positions thereby minimizing repulsive interactions. If now in a gedankenexperiment starting from the three most stable structures the two N atoms are pulled towards each other (downwards in Figure 3), which is what one could expect to happen during the process of iron(II) coordination, a boat conformation with N tips is obtained, and if the configuration at the ring atoms during this conformational change is kept, the *i*-butyl residues will finally end up in axial positions. Hence, a contact of $^{2i\text{-Bu}}$BPMP in its

most stable conformations with a metal centre would lead to a complex with a ligand conformation as shown in Figures 1 and 2. This would be a kinetic explanation for the axial positions of the *i*-butyl residues in the complexes **1** and **2**. Having obtained these theoretical results an NMR study concerning the conformations and dynamics of $^{2i\text{-Bu}}$BPMP in solution suggested itself. However, while it became evident that the molecular dynamics are slowed down on the NMR time scale, and that there are two equitable isomers differing from each other in the structure of the piperazine ring, the identity of the corresponding conformations could not be derived (by determination of NOEs and J values), as the decisive proton signals of the piperazine rings are overlapping in the ^{1}H NMR spectrum and cannot be separated sufficiently by cooling.

Calculations concerning the complex constitution [($^{2i\text{-Bu}}$BPMP)Fe(Cl)$_2$] surprisingly showed that these structures are also favoured thermodynamically: The diastereomer shown in Figure 1 lies 37.0 kJ/mol lower in energy than an isomer with the *i*-butyl groups in equatorial positions (compare Figure 4). Searching for the origin of this significant energy difference first of all the influence of the chloride ligands was addressed, which turned out to be negligible: Performing analogous calculations for the dication [($^{2i\text{-Bu}}$BPMP)Fe]$^{2+}$ yielded likewise an energetic preference for the axially substituted isomer. Hence, the argumentation has to concentrate on the ligand frame work.

Although one might expect the lone-pairs of the piperazine N atoms to exclusively point towards the Fe atom, a detailed natural bond orbital (NBO) analysis showed that there is significant electron density at the opposite side, too, and it further revealed a significant stabilization of both isomers by transfer of electron density from this part of the lone-pairs to σ* orbitals of adjacent C-H and C-C bonds (negative hyperconjugation). The extent of the stabilization is 33.4 kJ/mol higher for the diastereomer with the *i*-butyl groups in axial positions, thus explaining almost quantitatively its energetic favouritism. Analyzing the negative hyperconjugation in more detail we found that electron density is mainly transferred to antibonding orbitals of the σ bonds involving the three C atoms connected to each of the N atoms. One of these orbitals belongs to a σ(C-H) bond as part of the CH_2 group within the piperazine framework and the second one to a σ(C-H) bond originating from the CH_2 group that leads to the pyridyl moiety; for both isomers both of these bonds are found in similar orientations almost parallel to the lone-pair of the N atoms. The third bond starts at the C_{ring} atom wearing the *i*-butyl group in addition to one H atom, and here the conformation makes a difference: Either the σ(C-C) bond of the *i*-butyl group or the σ(C-H) bond is in axial position, pointing parallel to the lone-pair of the N atom thus allowing for hyperconjugation. The difference in stabilization energy by transfer of electron density to the σ*(C-C) or the σ*(C-H) orbital, respectively, amounts to 24.9 kJ/mol and this is the main reason for the thermodynamic preference of the axial orientation of the *i*-butyl groups.

Hence, the goal of stabilizing a boat conformation for BPMP-based ligands has been reached – for unexpected reasons – with the synthesis of $^{2i\text{-Bu}}$BPMP. This new ligand can be used to synthesize mononuclear complexes [($^{2i\text{-Bu}}$BPMP)Fe(X)$_2$] with varying co-ligands X, and within those the tetrapodal coordination mode of the $^{2i\text{-Bu}}$BPMP ligand should be retained in solution. With regard to the background provided in the introduction it now seemed interesting to test the complexes as catalysts for the oxidation of hydrocarbons with H_2O_2. Since it has been argued in case of other $LFeX_2$ systems that the TOFs are influenced by the co-ligands X [2], special attention was paid to a comparison of the catalytic activity of the chloride **1** with the triflate **2**. Furthermore, an analysis of the results for **1**/**2** against the background of those observed employing [(BPMP)Fe(OTf)$_2$], **I**, will indicate whether the unsubstituted complex **I** remains as it is under catalytic conditions.

Table 1 lists the product distributions observed in the [(L)Fe(X)$_2$]/H_2O_2/cyclooctene (L = BPMP, $^{2i\text{-Bu}}$BPMP; X = Cl, OTf) experiments. To facilitate comparison with published data [2,3e-f,10,11] the experimental conditions for the oxidation reactions were chosen to resemble those with TPA, which, however was also reinvestigated in this work as a benchmark under *identical* conditions (see Experimental Section). Reacting cyclooctene with H_2O_2 in the presence of **I** as a catalyst (ratio 1000:10:1) selectively yields cyclooctene oxide with a TON of 1.1 (see Table 1). This is in agreement with the previous finding that mononuclear iron(II) complexes containing tetradentate N donor ligands and two further labile ligands oriented in *trans* positions lead to alkane hydroxylation or olefin epoxidations, while a *cis*-arrangement enables olefin dihydroxylation [10]: while **1** with a Cl-Fe-Cl angle of 127.37(3)° is certainly a borderline case, the O-Fe-O angle of 155.67(7)° must be interpreted in terms of a trans orientation). The complexes with the *i*-butyl substituted BPMP ligand **1** and **2** show a somewhat higher activity: They epoxidize cyclooctene with a TON of 1.5 and 1.4, respectively and are thus in this respect more active than a comparable bispidine complex, while they are more than twice as active as a corresponding complex of the N4Py ligand (Table 1), which, however, is pentadentate. They are not as efficient as complexes with the tetradentate ligands TPA or BPMEN but more selective (Table 1). The observation that the conversion of cyclooctene to the oxide is higher for **1** than for **2** is surprising, since it contradicts the finding that catalyst activity increases with increasing lability of ligands X (chlorido ligands are certainly bound stronger than OTf ligands). The reasons are not clear yet and are pursued in future investigations. The fact that **1** and **2** exhibit significantly higher TONs than **I** might indeed indicate than **I** is not structurally stable in solution, as suspected.

Table 1. Oxidation of cyclooctene by H_2O_2 catalyzed by iron complexes.[a]

catalyst	D[b]	E[b]	D/E
[(BPMP)Fe(OTf)$_2$], **I**	-	1.1(1)	-
[($^{2i\text{-Bu}}$BPMP)Fe(Cl)$_2$], **1**	-	1.5(1)	-
[($^{2i\text{-Bu}}$BPMP)Fe(OTf)$_2$], **2**	-	1.4(1)	-
[Fe(TPA)(CH_3CN)$_2$]$^{2+}$	1.7(1)[c]	2.5(1)[c]	0.7[c]
[Fe(bispidine[d])]$^{2+}$[3e]	1.5(1)	1.0(1)	1.5
[Fe(TPA)(CH_3CN)$_2$]$^{2+}$ [2,3f,10,11]	4.0(2)	3.4(1)	1.2
[Fe(BPMEN)(CH_3CN)$_2$]$^{2+}$ [2,3f,10,11]	0.9(2)	7.5(6)	0.1
[Fe(N4Py)(CH_3CN)]$^{2+}$ [2,3f,10,11]	-	0.6(2)	-

[a] Yields expressed in mole products per mole iron (= TON), 10 equiv. H_2O_2, 1000 equiv. cyclooctene, reaction time 25 minutes under argon in acetonitrile at ambient temperature. [b] D = *cis*-cyclooctane-1,2-diol, E = cyclooctene oxide. [c] Values determined in this work for comparison under identical conditions; values determined previously [2,3f,10,11] differ somewhat, probably due to different dilution, temperature, oxidant delivery or work up procedure. [d] The bispidine ligand is shown in Chart 1.

Table 2. Crystal data and experimental parameters for the crystal structure analyses of **1** and **2**.

	1	**2**
formula	$C_{24}H_{36}Cl_2FeN_4$	$C_{26}H_{36}F_6FeN_4O_6S_2$
weight, g mol^{-1}	507.32	734.56
temp. K	180(2)	100(2)
wavelength, Å	0.71073	0.71073
crystal system	orthorhombic	monoclinic
space group	P 2_1 2_1 2_1	P 2_1
a, Å	10.932(2)	11.9834(4)
b, Å	14.244(2)	15.5024(4)
c, Å	16.303(2)	26.3318(9)
α, °	90	90
β, °	90	93.329(3)
γ, °	90	90
V, Å^3	2538.5(5)	4883.4(3)
Z	4	6
density, g cm^{-3}	1.327	1.499
$\mu(Mo_{K\alpha})$, mm^{-1}	0.823	0.671
F(000)	1072	2280
GoF	0.922	1.033
R_1 (I>2σ(I)]	0.0278	0.0364
wR_2 [all data]	0.0573	0.0829
$\Delta\rho_{min}/\Delta\rho_{max}$, e Å^{-3}	-0.309/0.270	-0.980/0.447

Conclusions

A route has been developed that starting from enantiomerically pure *S*-leucine allows for the stereoselective synthesis of 1,4-bis(2-pyridyl-methyl)piperazines containing *i*-butyl substituents in the 2- and 5-positions with an *S*,*S* configuration ($^{2i\text{-Bu}}$BPMP). While the present investigation has not been extended to other amino acids, in principal this should be possible, so that other diastereomerically pure, alkyl-substituted piperazine-based ligands should be accessible via this procedure. The bulky *i*-butyl residues destabilize the chair conformation of the piperazine unit that often poses problems in coordination chemistry as it antagonises a tetrapodal coordination of the ligand to just one metal centre. The results of DFT calculations suggest that the most stable conformations of $^{2i\text{-Bu}}$BPMP contain the piperazine ring in a distorted boat conformation with C atoms at the boat tips – not the N atoms as apparently their lone pairs would lead to significant repulsion. In these conformations $^{2i\text{-Bu}}$BPMP is pre-organised to coordinate FeX_2 units yielding complexes with the two butyl residues in axial positions, as observed experimentally. This – at first sight – quite peculiar finding can also be rationalised on a thermodynamic basis: Compared to the corresponding isomer with the residues in equatorial position – which is the one expected intuitively – the axial substitution leads to a stabilisation by 37.0 kJ/mol due to hyperconjugation effects. The FeX_2 complexes should thus be stable as such and solution, and they were tested as catalysts for the oxidation of cyclooctene with H_2O_2: **1** and **2** are moderately active catalysts that selectively lead to the epoxide, and the nature of the co-ligand X has only little influence. Interestingly the TONs reached by **1** and **2** are significantly higher than the TON observed for **I**, which could be due to their enhanced configurational stability.

Experimental Section

Quantum-chemical Calculations

All Density Functional Calculations were carried out using the Gaussian 03 program package [12]. Geometry optimizations were performed in redundant internal coordinates without imposing symmetry constraints using the B3LYP functional [13]. The 6-31G* basis set [14] was employed for the study of the uncomplexed $^{2i\text{-Bu}}$BPMP molecule and the TZVP basis set [15] for the Fe complexes. The program NBO 3.0 [16] as implemented in Gaussian 03 was used for subsequent Natural Bond Orbital analyses.

General Experimental Techniques

All manipulations were carried out in a glove-box, or else by means of Schlenk-type techniques involving the use of a dry argon atmosphere and dry, degassed and argon saturated solvents.

Microanalyses were performed on a Leco CHNS 932 elemental analyser. Infrared (IR) spectra were recorded in the region 4000 – 400 cm^{-1} using samples prepared as KBr pellets with a Digilab Excalibur

FTS 4000 FTIR-spectrometer. ^{1}H and $^{13}C\{^{1}H\}$ NMR spectra were recorded on a Bruker AV 400 spectrometer. The spectra were calibrated against the internal residual proton and natural abundance ^{13}C resonances of the deuterated solvent.

The crystals were mounted on a glass fiber and then transferred into the cold nitrogen gas stream of the diffractometer (Stoe IPDS for **1**; Stoe IPDS2T for **2**) using $Mo_{K\alpha}$ radiation, λ = 0.71073 Å, and the structures were solved by direct methods (SHELXS-97) [17] refined versus F^2 (SHELXL-97) [18] with anisotropic temperature factors for all non-hydrogen atoms (Table 2). All hydrogen atoms were added geometrically and refined isotropically by using a riding model.

The crystallographic data (apart from structure factors) of **1** and **2** were deposited at the Cambridge Crystallographic Data Centre as supplementary publication no. 728470 (**1**) and 728471 (**2**). Copies of the data can be ordered free of charge on application to CCDC, 12 Union Road, Cambridge CB2 1EZ (FAX: (+44)1223-336-033; E-mail: deposit@ccdc.cam.ac.uk).

Syntheses

$Fe(OTf)_2(CH_3CN)_2$ was prepared according to the literature procedure [19]. The synthesis of $[(BPMP)Fe(OTf)_2]$ is described elsewhere [5].

Boc-*S*-Leu-*S*-Leu-OMe

Boc-*S*-Leu-OH (5.78 g, 25.0 mmol), *S*-Leu-OMe · HCl (4.54 g, 25.0 mmol) and NEt_3 (2.63 g, 26.0 mmol) were dissolved in CH_2Cl_2 (80 ml) and N,N'-dicyclohexylcarbodiimide (5.37 g, 26.0 mmol) was added in portions at 0°C. The reaction mixture was stirred for 4 hours at 0°C and afterwards 12 hours at room temperature. During this period of time large amounts of a white solid formed. The reaction mixture was filtered and the residue was extracted with CH_2Cl_2 (twice, 30 ml). The solvent of the combined phases was removed in vacuum, which resulted in a white solid that was suspended in 100 ml diethyl ether. The mixture was filtered, and the residue was extracted with diethyl ether (twice, 30 ml). The combined diethyl ether phases were successively washed with HCl solution (2%, 30 ml), $NaHCO_3$ solution (4%, 30 ml) and NaCl solution (saturated, 30 ml). After drying with $MgSO_4$, the drying agent was filtered off, and the solvent was removed in vacuum. Boc-*S*-Leu-*S*-Leu-OMe (8.13 g, 22.7 mmol, 91%) could be obtained in form of a white solid. ^{1}H NMR ($CDCl_3$): δ = 0.91-0.95 (m, 12H, $CH(CH_3)_2$), 1.44 (s, 9H, $C(CH_3)_3$), 1.51-1.70 (m, 6H, $CH(CH_3)_2$, $CH_2CH(CH_3)_2$), 3.72 (s, 3H, OCH_3), 4.09 (m, 1H, NCH), 4.61 (d, 1H, O_2CNCH), 4.86 (d, 1H, NH), 4.61 (d, 1H, O_2CNH); ^{13}C NMR ($CDCl_3$): δ = 21.8, 23.8, 24.6, 24.7 ($CHCH_3$, $CH(CH_3)_2$), 28.2 ($C(CH_3)_3$), 41.5 ($CH_2CH(CH_3)_2$), 50.6, 52.3 (NCH, OCH_3), 172.2 ($COC(CH_3)_3$), 173.2 (NHCO).

***Cyclo*-*S*-Leu-*S*-Leu**

Boc-*S*-Leu-*S*-Leu-OMe (8.13 g, 22.7 mmol) was dissolved in formic acid (200 ml), and the solution was stirred at room temperature for two hours. Afterwards the solvent was removed in vacuum and the temperature was held below 30°C. The residue, a yellow oil, was dissolved in methanol (50 ml) and the solution was stirred for 5 minutes. Subsequently, all volatiles were removed in vacuum and the

residue was dissolved in a mixture of 2-butanol (250 ml) and toluene (150 ml). The solution was boiled for 3 hours and the solvent level maintained by addition of fresh 2-butanol. Afterwards the volume was concentrated to 100 ml and the reaction mixture was kept for 12 hours at 0°C. A white solid precipitated, which was filtered off, washed with petrol ether (3 times, 50 ml) and dried in vacuum. The petrol ether phases were concentrated, and after cooling to -30°C additional product (1.00 g, 4.42 mmol) precipitated, which was separated by filtration and combined with the residue of the washing procedure. This led to *cyclo*-*S*-Leu-*S*-Leu (3.84 g, 17.0 mmol, 75%) in form of a white solid.

^{1}H NMR ($CDCl_3$): δ = 0.94-0.99 (m, 12H, C*H*$_3$), 1.60 (m, 2H, C*H*$(CH_3)_2$), 1.80 (m, 4H, C*H*$_2$), 3.97 (m, 2H, NC*H*), 7.07 (s, 2H, N*H*); ^{13}C NMR ($CDCl_3$): δ = 21.1, 23.3 (*C*H_3), 24.2 (*C*H$(CH_3)_2$), 43.6 (*C*H_2CH$(CH_3)_2$), 53.3 (N*C*H), 169.1 (*C*O).

Elemental analysis: $C_{12}H_{22}N_2O_2$ (226.32); C 63.76 (calc. 63.68), H 9.42 (9.80), N 12.24 (12.38)%.

Cis-2,5-di-_i_-butylpiperazine

Cyclo-*S*-Leu-*S*-Leu (12.6 g, 55.7 mmol) and $NaBH_4$ (13.7 g, 362 mmol) were suspended in DME (400 ml), and after cooling to 0°C $TiCl_4$ (34.3 g, 181 mmol) was added dropwise. The reaction mixture was heated for 12 hours under reflux, and $NaBH_4$ (2.74 g, 72.4 mmol) and $TiCl_4$ (7.63 g, 40.2 mmol) were added. This procedure was repeated twice. Afterwards the mixture was carefully hydrolyzed with water (400 ml), made alkaline by the addition of NH_3 solution (25%) which led to the precipitation of huge amounts of a white solid precipitated. The suspension was extracted with CH_2Cl_2 (10 times, 50 ml), and the combined organic CH_2Cl_2 phases were dried over $MgSO_4$. Subsequently, they were separated from the drying agent and the solvent was removed in vacuum. *Cis*-2,5-di-*i*-butylpiperazine (9.61 g, 48.4 mmol, 87%) was obtained in form of pale yellow oil.

^{1}H NMR ($CDCl_3$): δ = 0.85-0.89 (m, 12H, C*H*$_3$), 1.17-1.48 (m, 4H, C*H*$_2$CH$(CH_3)_2$), 1.60 (m, 2H, C*H*$(CH_3)_2$), 1.71 (s, 2H, N*H*), 2.60-2.83 (m, 6H, NC*H*$_2$, NC*H*); ^{13}C NMR ($CDCl_3$): δ = 22.2, 23.0 (*C*H_3), 24.4 (*C*H$(CH_3)_2$), 40.9 (*C*H_2CH$(CH_3)_2$), 48.4 (N*C*H), 51.6 (N*C*H_2).

Cis-2,5-di-_i_-butyl-1,4-bis(2-pyridyl-methyl)piperazine, $^{2i\text{-}Bu}$BPMP

Cis-2,5-di-*i*-butylpiperazine (8.60 g, 43.4 mmol), 2-(chloromethyl)pyridine (22.1 g, 173.4 mmol) and NEt_3 (35.1 g, 347 mmol) were dissolved in acetonitrile (300 ml) and heated under reflux for 15 hours. Afterwards the reaction mixture was extracted with a NaOH solution (1 mol/l, 300 ml) and the organic phase was separated. After extraction of the aqueous phase with CH_2Cl_2 (5 times, 50 ml), the organic phases were combined, and dried with $MgSO_4$. Subsequent to filtration the solvent was removed in vacuum which resulted in a red brown oil. Diethyl ether (100 ml) was added to the oil and the resulting mixture was refluxed for 30 minutes. Afterwards the diethyl ether phase was separated from an oily residue. This procedure was repeated 3 times. The diethyl ether phases were combined and stirred in the presence of activated carbon (50 g) for one hour. The filtrate was then subjected to column chromatography which allowed for the separation of *cis*-2,5-di-*i*-butyl-1,4-bis(2-pyridyl-methyl)piperazine (9.37 g, 24.6 mmol, 57%) in form of a yellow oil.

^{1}H NMR ($CDCl_3$): δ = 0.75-0.84 (m, 12H, CH_3), 1.35-1.55 (m, 6H, CH_2CH(CH_3)$_2$, CH(CH_3)$_2$), 2.55 (m, 6H, NCH, NCH_2), 3.52, 4.01 (m, 4H, CCH_2), 7.13 (m, 2H, C^5H), 7.51 (m, 2H, C^3H), 7.64 (m, 2H, C^4H), 8.51 (m, 2H, C^6H); ^{13}C-NMR ($CDCl_3$): δ = 22.0, 23.8 (CH_3), 25.6 ($CH(CH_3)_2$), 36.8, 36.9 ($CH_2CH(CH_3)_2$), 54.1 (NCH), 57.2 (NCH_2), 60.0 (CCH_2), 121.7 (C^5), 122.5 (C^3), 136.2 (C^4), 148.9 (C^6), 160.5 (C^2).

Elemental analysis: $C_{24}H_{36}N_4$ (380.57); C 74.96 (calc. 75.74), H 9.51 (9.53), N 14.41 (14.72)%.

[($^{2i\text{-Bu}}$BPMP)Fe(Cl)$_2$], 1

A solution of $FeCl_2$ (83 mg, 0.65 mmol) in acetonitrile (5 ml) was added dropwise to a stirred solution of $^{2i\text{-Bu}}$BPMP (250 mg, 0.65 mmol) in acetonitrile (5 ml), which resulted in an orange yellow solution. Addition of diethyl ether (10 ml) then led to the precipitation of a pale yellow solid. The suspension was filtered and the residue was washed with diethyl ether (3 times, 2 ml). [($^{2i\text{-Bu}}$BPMP)Fe(Cl)$_2$] could be obtained in pure form after drying of the solid in vacuum (232 mg, 0.46 mmol, 70%)

Single crystals of [($^{2i\text{-Bu}}$BPMP)Fe(Cl)$_2$] could been grown by slow evaporation of the solvent from a solution in acetonitrile.

Elemental analysis: $C_{24}H_{36}Cl_2FeN_4$ (507.32); C 56.88 (calc. 56.82), H 7.35 (7.15), N 11.09 (11.04), Cl 14.03 (13.98)%. IR (KBr): 3049 m, 3018 m, 2960 vs, 2932 vs, 2872 vs, 1602 vs, 1571 s, 1469 vs, 1431 vs, 1371 s, 1343 w, 1293 s, 1243 w, 1218 w, 1172 s, 1151 s, 1121 s, 1099 m, 1051 s, 1008 vs, 934 m, 866 w, 829 w, 764 vs, 738 w, 691 w, 643 w, 618 w, 583 w, 531 m, 474 w, 416 m cm^{-1}.

[($^{2i\text{-Bu}}$BPMP)Fe(OTf)$_2$], 2

A solution of Fe(OTf)$_2$(CH_3CN)$_2$ (286 mg, 657 µmol) in acetonitrile (10 ml) was added to a solution of $^{2i\text{-Bu}}$BPMP (250 mg, 657 µmol) in acetonitrile (5 ml) which led to the formation of an orange pink solution. The solvent was removed in vacuum and the residue was washed with diethyl ether (three times, 5 ml). Afterwards drying in vacuum [($^{2i\text{-Bu}}$BPMP)Fe(OTf)$_2$] (458 mg, 624 µmol, 95%) was obtained in form of a salmon coloured solid.

Single crystals suitable for X-Ray could be grown by overlayering a solution of [($^{2i\text{-Bu}}$BPMP)Fe(OTf)$_2$] in acetonitrile with diethyl ether.

Elemental analysis: $C_{26}H_{36}F_6FeN_4O_6S_2$ (734.55); C 42.30 (calc. 42.51), H 5.00 (4.94), N 7.62 (7.63), S 9.04 (8.73)%. IR (KBr): 2961 s, 2933 m, 2874 m, 1610 s, 1573 w, 1488 m, 1470 m, 1443 m, 1389 w, 1370 m, 1316 vs, 1235 vs, 1211 vs, 1167 vs, 1119 w, 1102 w, 1057 m, 1023 vs, 991 w, 933 w, 865 w, 829 w, 787 w, 767 s, 694 w, 635 vs, 581 w, 570 w, 544 w, 516 m, 469 w, 422 m cm^{-1}.

General procedure for the catalytic cyclooctene oxidation

To a vigorously stirred solution of iron complex (7 µmol) and cyclooctene (7 mmol, distilled before use) in acetonitrile (10 ml, dried and degassed) a solution of H_2O_2 (70 µmol) in acetonitrile (1 ml, previously dried over $MgSO_4$, containing 2,3-dimethylnaphthalene and diphenyl ether as an internal standard) was continuously delivered over a period of 25 minutes at 25°C under argon. The solution

was stirred for a further 5 min after completion of H_2O_2 addition. To remove the iron Chelex 100 (400 mg) were added and the mixture was stirred for 15 minutes. A batch of the organic solution was analyzed via GC-MS/FID (Varian GC/MS 4000). The oxidation products were identified by means of their retention times and mass spectra. Cyclooctene oxide and *cis*-cyclooctane-1,2-diol were quantified by internal and external calibration.

Acknowledgments

We are grateful to the Fonds der Chemischen Industrie, the Bundesministerium für Bildung, Wissenschaft, Forschung und Technologie and the Dr. Otto Röhm Gedächtnisstiftung for financial support as well as to Bayer Services GmbH & Co. OHG, BASF AG and Sasol GmbH for the supply of chemicals. We also would like to thank P. Neubauer and B. Ziemer for crystal structure analyses and Robert Zitterbart for performing the oxidation reactions. Finally, we acknowledge inspiring discussions within the Cluster of Excellence "Unifying Concepts in Catalysis" funded by the DFG.

[1] a) L. Que, Jr., W. B. Tolman, *Nature* **2008**, *455*, 333; b) M. Costas, M. P. Mehn, M. P. Jensen, L. Que, Jr., *Chem. Rev.* **2004**, *104*, 939; c) X. Shan, L. Que, Jr., *J. Inorg. Biochem.* **2006**, *100*, 421; d) E. Y. Tshuva, S. J. Lippard, *Chem. Rev.* **2004**, *104*, 987.

[2] K. Chen, M. Costas, L. Que, Jr., *J. Chem. Soc., Dalton Trans.* **2002**, 672.

[3] a) J. Kim, R. G. Harrison, C. Kim, L. Que, Jr., *J. Am. Chem. Soc.* **1996**, *118*, 4373; b) M. H. Lim, J.-U. Rohde, A. Stubna, M. R. Bukowski, M. Costas, R. Y. N. Ho, E. Münck, W. Nam, L. Que, Jr., *Proc. Natl. Acad. Sci. USA* **2003**, *100*, 3665; c) K. Chen, L. Que, Jr., *Chem. Commun.* **1999**, 1375; d) G. Roelfes, M. Lubben, R. Hage, L. Que, Jr., B. L. Feringa, *Chem. Eur. J.* **2000**, *6*, 2152; e) J. Bautz, P. Comba, C. Lopez de Laorden, M. Menzel, G. Rajaraman, *Angew. Chem.* **2007**, *119*, 8213; *Angew. Chem. Int. Ed.* **2007**, *46*, 8067; f) M. R. Bukowski, P. Comba, A. Lienke, C. Limberg, C. Lopez de Laorden, R. Mas-Ballesté, M. Merz, L. Que, Jr., *Angew. Chem.* **2006**, *118*, 3524; *Angew. Chem. Int. Ed.* **2006**, *45*, 3446; g) M. R. Bukowski, P. Comba, C. Limberg, M. Merz, L. Que, Jr., *Angew. Chem.* **2004**, *116*, 1303; *Angew. Chem. Int. Ed.* **2004**, *43*, 1283.

[4] M. S. Chen, M. C. White, *Science* **2007**, *318*, 783.

[5] M. Ostermeier, C. Limberg, B. Ziemer, *Z. Anorg. Allg. Chem.* **2006**, *632*, 1287.

[6] a) J. Ratilainen, K. Airola, R. Fröhlich, M. Nieger, K. Rissanen, *Polyhedron* **1999**, *18*, 2265; b) J. A. Halfen, J. M.Uhan, D. C. Fox, M. P. Mehn, L. Que, Jr., *Inorg. Chem.* **2000**, *39*, 4913; c) J. M. J. Nuutinen, J. Ratilainen, K. Rissanen, P. Vainiotalo, *J. Mass. Spectrometr.* **2001**, *36*, 902.

[7] But compare: M. Ostermeier, C. Limberg, B. Ziemer, V. Karunakaran, *Angew. Chem.* **2007**, *119*, 5423; *Angew. Chem. Int. Ed.* **2006**, *46*, 5329.

[8] D. E. Nitecki, B. Halpern, J. W. Westley, *J. Org. Chem.* **1968**, *33*, 864.

[9] W. Langenbeck, M. Augustin, R. Böhm, S. Hoffmann, *J. Prakt. Chem.* **1964**, *25*, 301.

[10] K. Chen, L. Que, Jr., *Angew. Chem.* **1999**, *111*, 2365; *Angew. Chem. Int. Ed.* **1999**, *38*, 2227.

[11] K. Chen, M. Costas, J. Kim, A. K. Tipton, L. Que, Jr., *J. Am. Chem. Soc.* **2002**, *124*, 3026.

[12] Gaussian 03, Revision D.01, M. J. Frisch, G. W. Trucks, H. B. Schlegel, G. E. Scuseria, M. A. Robb, J. R. Cheeseman, J. A. Montgomery, Jr., T. Vreven, K. N. Kudin, J. C. Burant, J. M. Millam, S. S. Iyengar, J. Tomasi, V. Barone, B. Mennucci, M. Cossi, G. Scalmani, N. Rega, G. A. Petersson, H. Nakatsuji, M. Hada, M. Ehara, K. Toyota, R. Fukuda, J. Hasegawa, M. Ishida, T. Nakajima, Y. Honda, O. Kitao, H. Nakai, M. Klene, X. Li, J. E. Knox, H. P. Hratchian, J. B. Cross, V. Bakken, C. Adamo, J. Jaramillo, R. Gomperts, R. E. Stratmann, O. Yazyev, A. J. Austin, R. Cammi, C. Pomelli, J. W. Ochterski, P. Y. Ayala, K. Morokuma, G. A. Voth, P. Salvador, J. J. Dannenberg, V. G. Zakrzewski, S. Dapprich, A. D. Daniels, M. C. Strain, O. Farkas, D. K. Malick, A. D. Rabuck, K. Raghavachari, J. B. Foresman, J. V. Ortiz, Q. Cui, A. G. Baboul, S. Clifford, J. Cioslowski, B. B. Stefanov, G. Liu, A. Liashenko, P. Piskorz, I. Komaromi, R. L. Martin, D. J. Fox, T. Keith, M. A. Al-Laham, C. Y. Peng, A. Nanayakkara, M. Challacombe, P. M. W. Gill, B. Johnson, W. Chen, M. W. Wong, C. Gonzalez, and J. A. Pople, Gaussian, Inc., Wallingford CT, **2004**.

[13] a) A. D. Becke, *Phys. Rev. A* **1988,** *38*, 3098; b) C. Lee, W. Yang, and R. G. Parr, *Phys. Rev. B* **1988**, *37*, 785; c) A. D. Becke, *J. Chem. Phys.* **1993**, *98*, 5648.

[14] a) R. Ditchfield, W. J. Hehre, and J. A. Pople, *J. Chem. Phys.* **1971**, *54*, 724; b) R. C. Binning Jr. and L. A. Curtiss, *J. Comp. Chem.* **1990**, *11*, 1206; c) V. A. Rassolov, M. A. Ratner, J. A. Pople, P. C. Redfern, and L. A. Curtiss, *J. Comp. Chem.* **2001**, *22*, 976.

[15] a) A. Schaefer, H. Horn, R. Ahlrichs, *J. Chem. Phys.* **1992**, *97*, 2571; b) A. Schaefer, C. Huber, R. Ahlrichs, *J. Chem. Phys.* **1994**, *100*, 5829.

[16] a) J. E. Carpenter and F. Weinhold, *J. Mol. Struct. (Theochem)* **1988**, *169*, 41; b) A. E. Reed, L. A. Curtiss, and F. Weinhold*, Chem. Rev.* **1988**, *88*, 899.

[17] G. M. Sheldrick, SHELXS-97, Program for Crystal Structure Solution, University of Göttingen, **1997**.

[18] G. M. Sheldrick, SHELXL-97, Program for Crystal Structure Refinement, University of Göttingen, **1997**.

[19] a) R. A. Heintz, J. A. Smith, P. S. Szalay, A. Weisgerber, K. R. Dunbar, K. Beck, D. Coucouvanis, *Inorg. Synth.* **2002**, *33*, 75; b) A. M. Tait, D. H. Busch, *Inorg. Synth.* **1978**, *18*, 2.

Figure 1. Molecular structure of **1**. Hydrogen atoms are omitted for clarity. Selected bond lengths [Å] and angles [°]: Fe-Cl1 2.3876(8), Fe-Cl2 2.3499(7), Fe-N1 2.320(2), Fe-N2 2.284(2), Fe-N3 2.310(2), Fe-N4 2.293(2); Cl1-Fe-N1 84.70(6), Cl1-Fe-N2 88.91(6), Cl1-Fe-N3 131.84(5), Cl1-Fe-N4 93.33(5), Cl1-Fe-Cl2 127.37(3), Cl2-Fe-N1 88.90(5), Cl2-Fe-N2 87.13(5), Cl2-Fe-N3 95.53(5), Cl2-Fe-N4 132.90(5), N1-Fe-N2 168.23(7), N1-Fe-N3 120.96(7), N1-Fe-N4 70.39(7), N2-Fe-N3 70.50(7), N2-Fe-N4 119.97(7), N3-Fe-N4 64.13(7).

Figure 2. Molecular structure of **2**. Hydrogen atoms are omitted for clarity. Selected bond lengths [Å] and angles [°]: Fe-O1 2.167(2), Fe-O2 2.174(2), Fe-N1 2.154(2), Fe-N2 2.200(2), Fe-N3 2.308(2), Fe-N4 2.203(2); O1-Fe-N1 92.19(7), O1-Fe-N2 82.07(7), O1-Fe-N3 111.69(7), O1-Fe-N4 89.98(7), O1-Fe-O2 155.67(7), O2-Fe-N1 86.28(7), O2-Fe-N2 86.36(7), O2-Fe-N3 85.64(7), O2-Fe-N4 113.17(7), N1-Fe-N2 147.83(8), N1-Fe-N3 135.22(7), N1-Fe-N4 76.75(7), N2-Fe-N3 75.21(8), N2-Fe-N4 134.50(7), N3-Fe-N4 66.42(7).

Figure 3. The three most stable and the least stable isomer of $^{2i\text{-Bu}}$BPMP as found by DFT calculations (B3LYP/6-31G*, singlet state). H atoms are shown at the piperazine ring only. Numbers are the total energies in kJ/mol relative to the first (most stable) isomer.

Figure 4. Optimized structures of [($^{2i\text{-Bu}}$BPMP)Fe(Cl)$_2$] with *i*-butyl groups in axial and equatorial position, respectively, according to the results of DFT calculations (B3LYP/TZVP, quintet state). Hydrogen atoms are omitted for clarity. Bond lengths for the diastereoisomer in Fig. 1 deviate by 0.001-0.03 Å only, apart from Fe-N3 and Fe-N4 (both 2.436 Å); angles [°] deviate by 0.2-3°, apart from Cl1-Fe-N3 126.50, Cl1-Fe-N4 91.19, Cl1-Fe-Cl2 138.08, Cl2-Fe-N3 91.19, Cl2-Fe-N4 126.50, N1-Fe-N2 171.57.

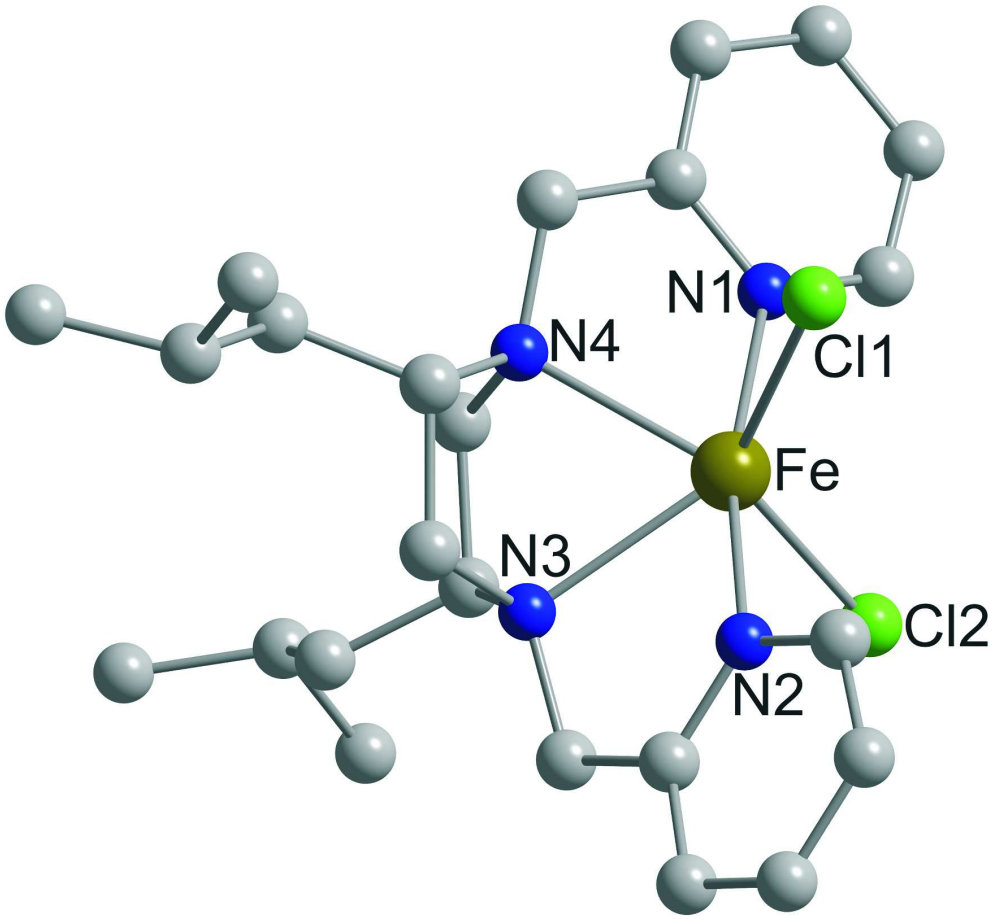

149x138mm (600 x 600 DPI)

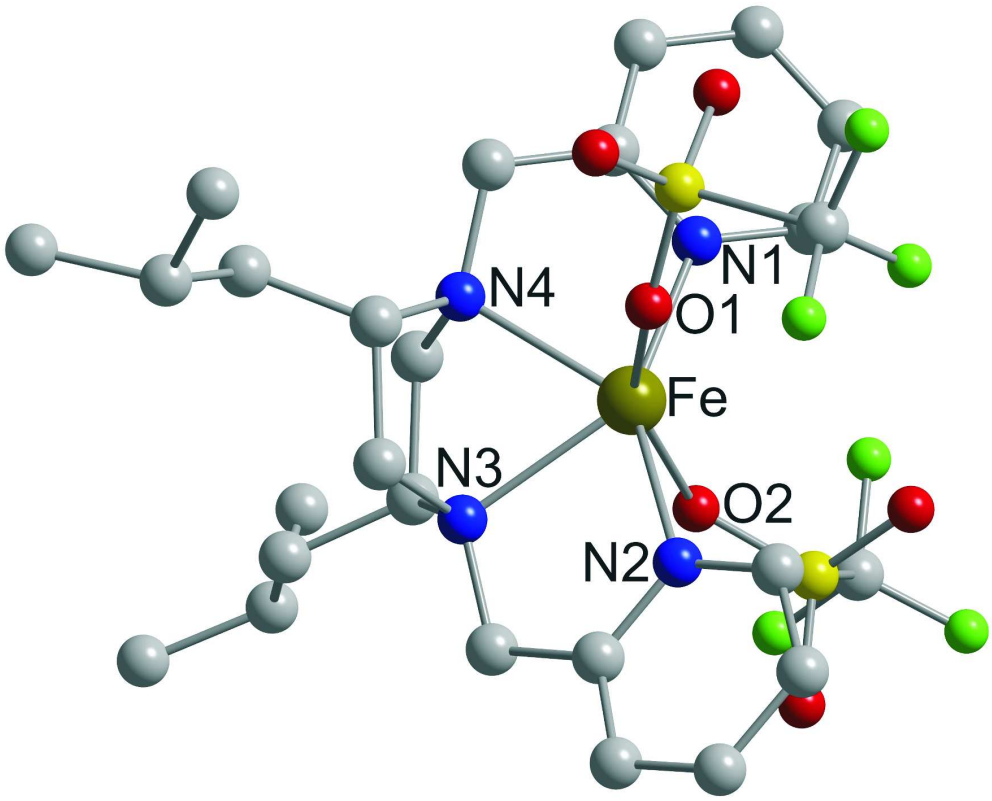

149x120mm (600 x 600 DPI)

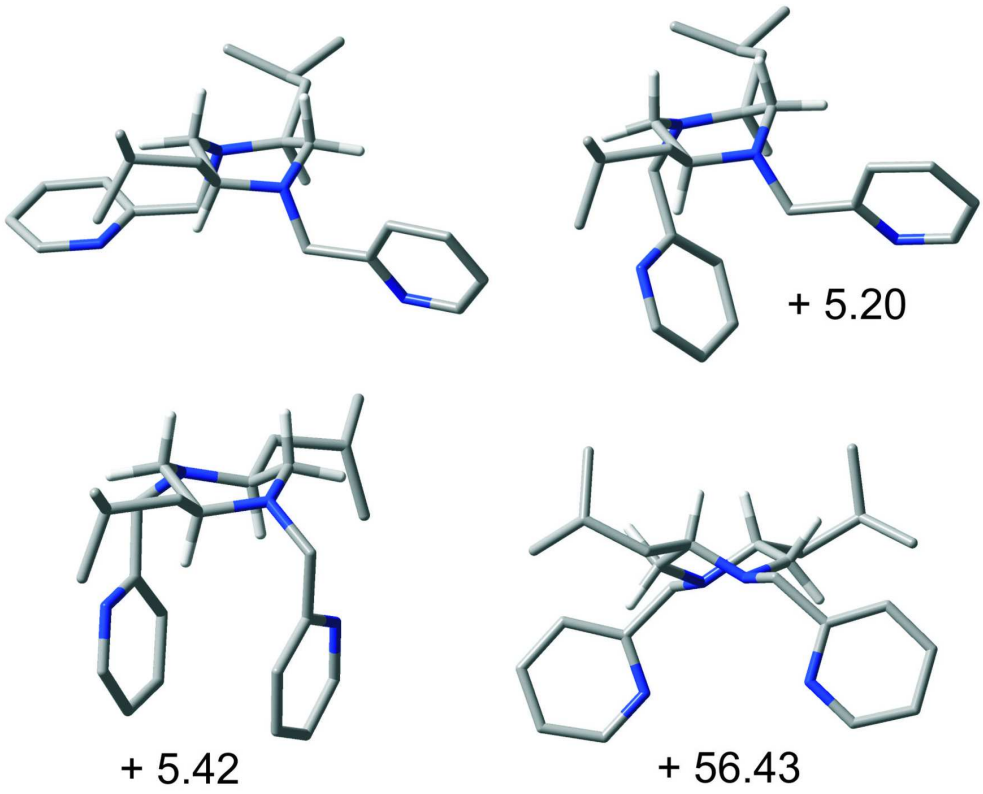

149x120mm (600 x 600 DPI)

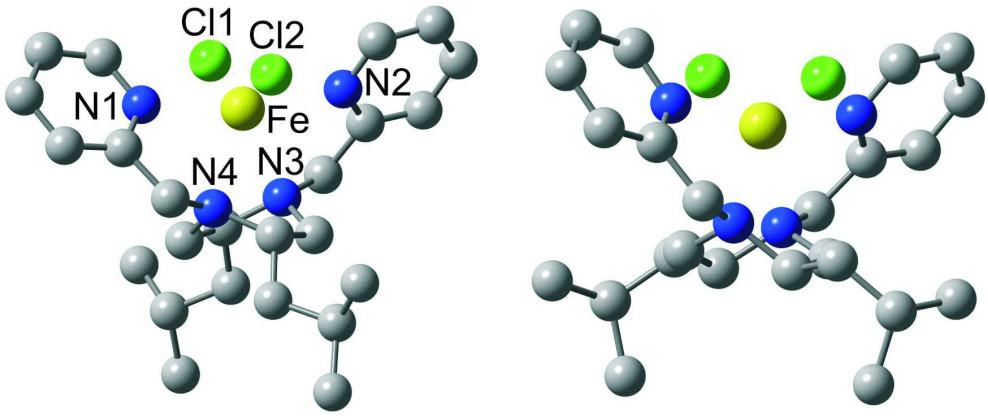

149x63mm (600 x 600 DPI)